






# The leaf economics spectrum of triploid and tetraploid C<sub>4</sub> grass *Miscanthus x giganteus*

Shuai Li<sup>1,2,3</sup>  | Christopher A. Moller<sup>2,4</sup> | Noah G. Mitchell<sup>2,4</sup> |  
 Duncan G. Martin<sup>1,5</sup> | Erik J. Sacks<sup>1,6</sup>  | Sampurna Saikia<sup>6</sup> |  
 Nicholas R. Labonte<sup>1,6</sup> | Brian S. Baldwin<sup>7</sup> | Jesse I. Morrison<sup>7</sup> |  
 John N. Ferguson<sup>2,8</sup>  | Andrew D. B. Leakey<sup>1,2,5</sup>  | Elizabeth A. Ainsworth<sup>1,2,4,5</sup> 

<sup>1</sup>Center for Advanced Bioenergy and Bioproducts Innovation, University of Illinois at Urbana-Champaign, Urbana, Illinois, USA

<sup>2</sup>Carl R. Woese Institute for Genomic Biology, University of Illinois at Urbana-Champaign, Illinois, Urbana, USA

<sup>3</sup>Institute for Sustainability, Energy, and Environment, University of Illinois at Urbana-Champaign, Urbana, Illinois, USA

<sup>4</sup>Global Change and Photosynthesis Research Unit, USDA ARS, Urbana, Illinois, USA

<sup>5</sup>Department of Plant Biology, University of Illinois at Urbana-Champaign, Urbana, Illinois, USA

<sup>6</sup>Department of Crop Sciences, University of Illinois at Urbana-Champaign, Urbana, Illinois, USA

<sup>7</sup>Department of Plant and Soil Sciences, Mississippi State University, Starkville, Mississippi, USA

<sup>8</sup>Department of Plant Sciences, University of Cambridge, Cambridge, UK

## Correspondence

Elizabeth A. Ainsworth, Global Change and Photosynthesis Research Unit, USDA ARS, 1201 W. Gregory Dr, 147 ERML, Urbana, IL 61801, USA.

Email: [lisa.ainsworth@ars.usda.gov](mailto:lisa.ainsworth@ars.usda.gov)

## Funding information

DE-SC0018420; U.S. Department of Energy

## Abstract

The leaf economics spectrum (LES) describes multivariate correlations in leaf structural, physiological and chemical traits, originally based on diverse C<sub>3</sub> species grown under natural ecosystems. However, the specific contribution of C<sub>4</sub> species to the global LES is studied less widely. C<sub>4</sub> species have a CO<sub>2</sub> concentrating mechanism which drives high rates of photosynthesis and improves resource use efficiency, thus potentially pushing them towards the edge of the LES. Here, we measured foliage morphology, structure, photosynthesis, and nutrient content for hundreds of genotypes of the C<sub>4</sub> grass *Miscanthus x giganteus* grown in two common gardens over two seasons. We show substantial trait variations across *M. x giganteus* genotypes and robust genotypic trait relationships. Compared to the global LES, *M. x giganteus* genotypes had higher photosynthetic rates, lower stomatal conductance, and less nitrogen content, indicating greater water and photosynthetic nitrogen use efficiency in the C<sub>4</sub> species. Additionally, tetraploid genotypes produced thicker leaves with greater leaf mass per area and lower leaf density than triploid genotypes. By expanding the LES relationships across C<sub>3</sub> species to include C<sub>4</sub> crops, these findings highlight that *M. x giganteus* occupies the boundary of the global LES and suggest the potential for ploidy to alter LES traits.

## KEYWORDS

C<sub>4</sub> photosynthesis, genotypic variation, leaf mass per area, Ploidy

This is an open access article under the terms of the Creative Commons Attribution-NonCommercial-NoDerivs License, which permits use and distribution in any medium, provided the original work is properly cited, the use is non-commercial and no modifications or adaptations are made.

© 2022 The Authors. *Plant, Cell & Environment* published by John Wiley & Sons Ltd. This article has been contributed to by US Government employees and their work is in the public domain in the USA

## 1 | INTRODUCTION

The leaf economics spectrum (LES) describes striking relationships among leaf functional traits and reflects fundamental trade-offs that underpin key ecological strategies for resource acquisition and use in plants (Reich et al., 1997; Wright et al., 2004). Fast-growing species are characterized by a quick potential rate of return on leaf nutrients and dry mass investments with low leaf mass per unit area (LMA), high nitrogen and phosphorus content per unit leaf mass ( $N_m$  and  $P_m$ , respectively), and high rates of respiration and photosynthesis per unit dry mass ( $R_m$  and  $A_m$ , respectively). In contrast, slow-growing species with the opposite traits have high LMA, low  $N_m$ ,  $P_m$  and  $A_m$  representing a slow return on investment of resources (Reich, 2014; Wright et al., 2005). Initially, the LES explained across-species variation in leaf morphology and function in a broad diversity of species found in their natural ecosystems (Wright et al., 2004). However, an increasing number of studies revealed variability in leaf functional traits and trait relationships within species and large discrepancies between the global LES and within-species trait data (Albert et al., 2010; Anderegg et al., 2018; Blonder et al., 2013, 2015; Niinemets, 2015). Recent studies also demonstrated that crops in agroecosystems tend to deviate from the general pattern of the global LES (Hayes et al., 2019; Martin et al., 2017, 2018; Xiong & Flexas, 2018). However, these studies used data compiled from global and regional databases covering a wide range of climatic conditions and failed to distinguish between genetic and phenotypic plasticity of trait variation.

Strong trait variation within or across species is both a consequence of plastic responses to environmental gradients and evolutionary genetic changes. For example, polyploidy or whole genome duplication, often contributes to dramatic changes in leaf morphology and physiology and confers enhanced tolerance to biotic and abiotic stress and adaptation to capricious or novel environments (Chao et al., 2013; Soltis & Soltis, 2000). Studies demonstrate that leaf size and thickness, stomatal size and photosynthesis often increase with polyploidy in both  $C_3$  and  $C_4$  species (Baker et al., 2017; Hao et al., 2013; Masterson, 1994; Vyas et al., 2007; Warner & Edwards, 1989; Warner et al., 1987). Tetraploids exhibit higher uptake of potassium (K) than diploids in *Arabidopsis* (Chao et al., 2013). Bagheri and Mansouri (2015) reported calcium (Ca) and phosphorus (P) concentrations were significantly increased and sulphur (S) content was decreased in tetraploid cannabis (*Cannabis sativa* L.) leaves compared with their diploid counterparts. These studies suggest polyploidization plays a substantial and overlooked role in plant resource use strategy, and, as a result, in coordination of leaf functional traits. A better understanding of the effect of polyploidy on leaf traits and trait relationships within species requires common garden experiments that highlight the genetic contribution to phenotypes found when plants are grown in identical environments.

While the global LES explains the trade-offs of leaf functional traits in  $C_3$  species, co-variation in leaf chemical, structural and physiological properties in  $C_4$  species has been largely unstudied.  $C_4$

plants comprise ~3% of land plant species, but account for nearly 25% of global terrestrial primary productivity (Sage et al., 1999; Still et al., 2003).  $C_4$  plants are widely distributed from the tropics to the warm-temperate zone within 50° of the Equator and dominate grasslands and savannas in these regions (Ehleringer et al., 1997; Still et al., 2003).  $C_4$  plants include major sources of food and biofuels worldwide, such as maize (*Zea mays*), sorghum (*Sorghum bicolor*) and Miscanthus (Heaton et al., 2008; Lewandowski et al., 2000; Ranum et al., 2014; Rooney et al., 2007). Therefore, the lack of  $C_4$  leaf traits in the global LES limits our understanding of overall plant functional strategies and ecosystem function.  $C_4$  photosynthesis involves a series of anatomical and biochemical modifications to concentrate  $CO_2$  around Rubisco. Most  $C_4$  leaves are characterized by Kranz anatomy, in which mesophyll cells surround bundle sheath cells and bundle sheath cells further surround the vascular bundle (Hatch, 1987; Sage, 2004). The initial fixation of atmospheric  $CO_2$  occurs in mesophyll cells by phosphoenolpyruvate carboxylase (PEPCase), followed by decarboxylation and refixation of  $CO_2$  by Rubisco in bundle sheath cells (Hatch, 1987; Sage, 2004). Higher activity of PEPCase effectively concentrates  $CO_2$ , leading to a high  $CO_2/O_2$  ratio around Rubisco, thereby increasing photosynthetic efficiency and decreasing photorespiration (Ehleringer & Monson, 1993).  $C_4$  species typically exhibit superior efficiencies of carbon fixation, water and nutrient use, and increased resistance to environmental stress compared to  $C_3$  species (Ehleringer & Monson, 1993; Leakey et al., 2019; Li et al., 2022; Montes et al., 2022). As a result, multivariate correlations among leaf functional traits in  $C_4$  species may not be consistent or may differ greatly from the general trends observed in the global fundamental leaf trait relationships.

In this study, we collected leaf functional traits from more than 200 genotypes of *Miscanthus* × *giganteus* grown in two common garden experiments in 2018 and 2019. *Miscanthus*, a tall and high-yielding perennial  $C_4$  grass which originated in East Asia, was successfully introduced and cultivated in North America and in Europe in the second half of the 19th century (Clark et al., 2015, 2019; Lewandowski et al., 2000; Quinn et al., 2010). *M.* × *giganteus* is a highly productive interspecific hybrid of tetraploid *Miscanthus sacchariflorus* and diploid *Miscanthus sinensis* and has been widely recognized as an emerging and promising feedstock for bioenergy production (Heaton et al., 2008; Hodkinson et al., 2002; Hodkinson & Renvoize, 2001; Lewandowski et al., 2000). Owing to its low nutrient requirements and high water-use efficiency, *M.* × *giganteus* can produce high biomass yields across a variety of soil and climatic conditions on marginal lands without competing with food crops (Clifton-Brown et al., 2017; Lewandowski et al., 2000). *M.* × *giganteus* genotypes display considerable phenotypic variation, which exists within and between cultivars and an abundant cytotype diversity that ranges in ploidy from diploid to hexaploid (Clark et al., 2019; Głowacka et al., 2015). Therefore, *M.* × *giganteus* is an excellent model for exploring the LES in  $C_4$  species. Specifically, we ask the following questions: (1) what is the genotypic range of leaf functional traits in *M.* × *giganteus*? (2) to what extent do the traits and relationships change with ploidy levels? (3) is the  $C_4$  LES trait covariation consistent with the general pattern of the global LES?

## 2 | METHODS AND MATERIALS

### 2.1 | Site description

This study was conducted in 2018 and 2019 at the Energy Farm (EF) (referred to as 2018 IL and 2019 IL, respectively) of University of Illinois in Urbana, Illinois (40°03'56"N, 88°12'21"W, elevation 219 m) and in 2019 at the Mississippi Agricultural and Forestry Experiment Station (MAFES) (referred to as 2019 MS) of Mississippi State University in Starkville, Mississippi (33°23'43"N, 88°44'31"W, elevation 56 m). The EF receives an average of 1009 mm of rainfall per year (30-year average, 1981–2010, data from <https://www.ncdc.noaa.gov/cdo-web/datatools/normals>) with ca. 50% falling during the growing season from May to September. The mean annual temperature is 10.9°C ranging from a mean monthly winter minimum of -8.2°C to a mean monthly summer maximum of 29.0°C. At EF, the 2018 and 2019 growing seasons (May–September) experienced total rainfall of 523.7 and 455.4 mm, respectively, and slightly higher air temperatures than observed historically. The soils at EF are Mollisols with Dana silt loams, Drummer silty clay loams, and Flanagan silt loams texture (Soil Survey Staff, 2015). At MAFES, long-term (1981–2010) mean annual precipitation is ~1403 mm, of which 871 mm falls from March to October, and the mean annual temperature is 16.9°C with a minimum of -0.67°C in winter and a maximum of 33.1°C in summer (<https://www.ncdc.noaa.gov/cdo-web/datatools/normals>). However, the 2019 growing season (March–October) receives total precipitation of 1587 mm which was considerably above the 30-year mean. Soil type at MAFES is Kipling silty clay loam.

### 2.2 | Plant materials

Field trials were established on 18–19 June 2018 at EF, and on 8–11 October 2018 at MAFES. Each *M.× giganteus* genotype was vegetatively propagated by planting rhizome divisions into 72-cell trays (T.O. Plastics, Clearwater) and grown in a greenhouse before planting in the field. The field trials were randomized complete block designs with three replications at each site. Plots consisted of single rows of eight plants spaced 0.91 m within and between rows. At the EF, the aboveground portions of all plants were maintained over the winter of 2018–2019 and removed in the spring of 2019 before tiller emergence. However, 49 genotypes were damaged and not available at EF in 2019 due to poor overwintering ability (Dong et al., 2019). In total, 216 genotypes were studied at EF in 2018 and 167 genotypes in 2019; at MAFES 202 genotypes were studied in 2019 (Supporting Information: Table S1). Among these, 167 genotypes were studied at EF in both 2018 and 2019, 180 genotypes were measured at both EF in 2018 and MAFES in 2019, and 141 genotypes were studied at both EF and MAFES in 2019 (Supporting Information: Table S1). Hence, 141 genotypes were measured at both EF and MAFES in both years (Supporting Information: Table S1).

### 2.3 | Ploidy assessment

Flow cytometry was used to determine DNA content and infer ploidy following previously described protocols (Chae, 2012; Clark et al., 2015; Rayburn et al., 2009). Briefly, using a razor blade, 1 cm<sup>2</sup> samples of young fully emerged leaves of each *Miscanthus* genotype were co-chopped with 1 cm<sup>2</sup> leaf samples of *S. bicolour* as an internal standard in an extraction buffer consisting of 10 mM Tris, 10 mM MgCl<sub>2</sub>, 0.5% Triton X-100, 13% hexylene glycol. Extracts were passed through 50 μm nylon filters and kept on ice before centrifugation at 2100 RPM for 20 min at 4°C. Pellets were resuspended in 300 μl of propidium iodide (Sigma-Aldrich) stain, then incubated at 37°C for 20 min in the dark. Following incubation, 300 μl of propidium iodide salt solution was added to each tube and stored on ice in the dark for at least 1 h. A minimum of 20 000 nuclei per sample were analyzed on a flow cytometer (model BD LSR II, BD Biosciences) at the Roy J. Carver Biotechnology Center (<https://biotech.illinois.edu/cmto/services-equipment>). The excitation wavelength was set to 488 and a 570 nm emission filter was used. The mean fluorescence of the *Miscanthus* G1 peak was divided by the G0/G1 peak of sorghum, multiplied by 1.74 pg/2C and expressed in pg/2C nucleus. DNA contents were estimated for known diploid *M. sinensis*, tetraploid *M. sacchariflorus* (including the parents of the *M.× giganteus* progenies if available), and triploid and tetraploid *M.× giganteus* genotypes, which were used as references for inferring ploidy of *M.× giganteus* genotypes for which estimates had not previously been obtained.

We were unable to identify ploidy levels in group 14UI-037 due to very low DNA content (Supporting Information: Table S1). Group 14UI-037 is a hybrid between tetraploid *M. sacchariflorus* 'Hokkaido Univ-selection-1' and diploid *M. sinensis* 'Silberturm (Silver Tower)', and has 59 genotypes in total. Additionally, the ploidy levels of 22 genotypes measured at EF and MAFES in both years were undetermined. In this study, two genotypes (UI10-00110 at EF and 14UI-016R.020 at MAFES) were identified as pentaploid and four genotypes (UI10-00109, UI10-00111, UI10-00114 and UI10-00115) at EF were identified as hexaploid (Supporting Information: Table S1). Therefore, only triploid and tetraploid genotypes at both sites and years were included in the analysis of ploidy level effect on variation in leaf traits and LES. In sum, 97 triploid and 35 tetraploid genotypes were studied at EF in 2018, 90 triploids and 27 tetraploids were studied at EF in 2019, and 89 triploid and 40 tetraploid genotypes were measured at MAFES in 2019 (Supporting Information: Table S1).

### 2.4 | Phenotyping

The leaf physiological and morphological measurements at EF were carried out in September of 2018 and 2019, and the measurements at MAFES were performed in July 2019. To avoid the potential influence of leaf age on trait values (Mason et al., 2013; McKown et al., 2013), we selected the youngest fully expanded sun-exposed leaves, typically the third or fourth leaf from the shoot apex, for the measurements. One or

two leaves from each of one or two individuals per genotype in each block were randomly selected and sampled, and the same leaf was used for all physiological, morphological and nutrient measurement.

### 2.4.1 | Gas exchange

Simultaneous gas-exchange and chlorophyll fluorescence were measured in the field using infrared gas analyzers in 2018 (LI-6400XT, LICOR Biosciences) and in 2019 (LI-6800, LICOR Biosciences). Both LI-6400XT and LI-6800 were equipped with a 2 cm<sup>2</sup> chlorophyll fluorometer chamber. All measurements at EF and MAEFS were performed on sunny days between 9.00 and 14.00 h, at a photosynthetic photon flux density (PPFD) of 1800–1900 μmol m<sup>-2</sup> s<sup>-1</sup> and relative humidity between 60% and 70%. Leaf temperatures ranged from 29 to 36°C at EF, and from 34 to 38°C at MAEFS. CO<sub>2</sub> concentration within the block was maintained at 410 μmol mol<sup>-1</sup> in 2018 and 420 μmol mol<sup>-1</sup> in 2019. Area-based leaf maximum photosynthetic rate ( $A_a$ , see Supporting Information: Table S2 for abbreviations) and stomatal conductance ( $g_{sa}$ ) were recorded after stabilization of gas exchange rates. The leaf was further illuminated with a saturating irradiance (ca. 10000 μmol m<sup>-2</sup> s<sup>-1</sup> PPFD) to determine chlorophyll fluorescence including quantum yield of PSII ( $\Phi_{PSII}$ ), electron transport rate (ETR), PSII maximum efficiency ( $F_v'/F_m'$ ), and coefficient of photochemical quenching ( $qP$ ). Instantaneous water use efficiency (iWUE, μmol mol<sup>-1</sup>) was calculated from  $iWUE = A_a/g_{sa}$ .

### 2.4.2 | Leaf morphology and LMA

Following gas exchange measurements, the same leaf was used to measure leaf area ( $L_a$ , cm<sup>2</sup>), length ( $L_l$ , cm) and width ( $L_w$ , cm) with a portable leaf area metre (LI-3000C, LICOR Biosciences). We further estimated leaf chlorophyll concentration with a portable chlorophyll metre (SPAD 502; Minolta corporation, Ltd) and leaf thickness ( $T_{leaf}$ , μm) with a low-force micrometre (MDH-1"MB, Mitutoyo Co). For each leaf, 6–8 readings were taken across the lamina and the average value was recorded. SPAD values were measured in 2019 at EF and MAEFS. All leaves in both years and locations were then harvested and dried at 70°C for at least 72 h. LMA was calculated as leaf dry mass divided by leaf area. Leaf density ( $\rho_{leaf}$ , g cm<sup>-3</sup>) was calculated as  $LMA/T_{leaf}$  (Witkowski & Lamont, 1991). LMA was then used to derive mass-based photosynthetic rates ( $A_m$ , nmol g<sup>-1</sup> s<sup>-1</sup>) and stomatal conductance ( $g_{sm}$ , mol g<sup>-1</sup> s<sup>-1</sup>) by  $A_a$  and  $g_{sa}$ , respectively, divided by LMA.

### 2.4.3 | Nutrient content

Dried leaves were ground into a fine powder using a 2000 Geno/Grinder (Spex Sample Prep) for 10 min at 2000 stroke/min, and 3 mg of leaf tissue was weighed and analysed for mass-based leaf carbon ( $C_m$ ) and nitrogen ( $N_m$ ) concentrations using a Costech 4010 elemental analyzer (Costech Analytical Technologies, Inc). Leaf C:N ratio was calculated from  $C:N = C_m/N_m$ . Mass-based phosphorus

content was measured in triploid and tetraploid samples in 2019 with 61 triploids and 25 tetraploids at EF, and 58 triploids and 25 tetraploids at MAEFS by using inductively coupled plasma optical emission spectroscopy (ICP-OES, OPTIMA 3300 DV, Perkin-Elmer) after nitric acid digestion. Nutrient concentrations per unit area were calculated by multiplying mass-based nutrient concentrations by LMA. Photosynthetic nitrogen and phosphorus use efficiency ( $A_N$  and  $A_P$ ) were calculated as  $A_m$  divided by  $N_m$  and mass-based phosphorus concentration ( $P_m$ ), respectively.

## 2.5 | Statistical analyses

All statistical analyses were performed on the R platform (version 4.0.3) using the mean trait values of each genotype except analyses in Supporting Information: Table S4 which were done using individual values of LES traits. Trait differences between different sites and years, and between triploid and tetraploid genotypes at each site and year were compared by analysis of variance (one-way analysis of variance [ANOVA]) followed by Tukey's post hoc test. LES trait data was also explored using two-way ANOVA analyses to confirm variances associated with genotypic versus phenotypic plasticity. Correlations among leaf traits for all *M. × giganteus* data pooled and for different subset data were analyzed on a mass and an area basis using the Pearson's correlation analysis with the R package *corrplot*. The slope and intercept of bivariate relationships of key leaf traits were calculated with standardized major axis (SMA) analysis using the 'sma' function of the *smatr* R package (Warton et al., 2012). To understand how different ploidy levels altered the intraspecific leaf trait relationships and where *M. × giganteus* leaf traits fell within the global LES, the differences in the slope and intercept of bivariate relationships of key leaf traits were compared between triploid and tetraploid genotypes and between *M. × giganteus* and the global LES data set (Gloplnet database) using SMA. To further assess the contribution of site, year and ploidy level effects on multivariate trait relationships and covariation, SMA was also performed independently for each site and year. Although the Gloplnet data set comprised 2548 species, only 23 *C*<sub>4</sub> species with three species having the full range of leaf traits (LMA, photosynthesis, N and P content) were included (Wright et al., 2004). As such, the entire set of Gloplnet data was used for all analyses. To further test whether the distribution in *M. × giganteus* was similar to other *C*<sub>4</sub> energy crops and different from the global LES, we compared the range of traits in *M. × giganteus* with data from 869 photoperiod-sensitive *S. bicolor* lines (Ferguson et al., 2021). All data were log<sub>10</sub>-transformed before SMA analyses.

## 3 | RESULTS

### 3.1 | Genotypic leaf trait variation

Leaf traits varied spectacularly among *M. × giganteus* genotypes. Across all sites and years, leaf morphological traits (leaf area,  $L_a$ ; leaf length,  $L_l$ ; and leaf width,  $L_w$ ; see all abbreviations in Supporting Information: Table S2)

**TABLE 1** Key foliage traits measured in *Miscanthus × giganteus* in this study and comparison of *M. × giganteus* with *Sorghum bicolor* and Glopnet

Trait	<i>M. × giganteus</i>		<i>S. bicolor</i>		Glopnet	
	Range	Mean	Range	Mean	Range	Mean
LMA	41.0–99.6	67.1	29.2–43.2	34.5	14.4–1509.5	127.7
$A_a$	6.6–41.0	23.7	19.8–35.0	28.0	1.0–42.0	11.5
$A_m$	93.3–758.2	369.8	550.1–1019.3	812.5	4.8–662.3	127.8
$g_{sa}$	0.046–0.507	0.189	0.17–0.41	0.25	0.035–2.272	0.310
$g_{sm}$	0.53–6.85	2.92	4.8–12.3	7.3	0.062–44.719	3.299
iWUE	72.6–227.8	136.8	107.5–150.8	128.8	6.5–172.7	50.7
$N_a$	0.80–2.41	1.45	0.76–1.98	1.30	0.26–9.14	1.94
$N_m$	1.1–3.2	2.2	2.39–4.25	3.49	0.25–6.36	1.93
C:N	14.4–42.9	21.7	9.4–17.2	12.5	-	-
$P_a$	0.087–0.293	0.171	-	-	0.02–0.88	0.13
$P_m$	0.071–0.157	0.110	-	-	0.01–0.60	0.11
$A_N$	5.41–35.0	16.9	25.8–37.2	23.5	0.63–25.55	6.37
$A_P$	0.051–0.506	0.227	-	-	0.01–1.02	0.24
Reference	Present study		Ferguson et al., 2021		Wright et al., 2004	

Note: Trait abbreviations and units of measurement are provided in Supporting Information: Table S2. Further details about other leaf traits in *M. × giganteus* are given in Supporting Information: Table S3. Dashes (-) represent unavailable data.

Abbreviations:  $A_a$ , maximum photosynthetic rate per unit leaf area;  $A_m$ , maximum photosynthetic rate per unit leaf dry mass;  $A_N$ , photosynthetic nitrogen use efficiency;  $A_P$ , photosynthetic phosphorus use efficiency; C:N, leaf carbon-to-nitrogen ratio;  $g_{sa}$ , stomatal conductance per unit leaf area;  $g_{sm}$ , stomatal conductance per unit leaf dry mass; iWUE, instantaneous water-use efficiency; LMA, leaf mass per unit area;  $N_a$ , nitrogen concentrations per unit leaf area;  $N_m$ , nitrogen concentration per unit leaf dry mass;  $P_a$ , phosphorus concentration per unit leaf area;  $P_m$ , phosphorus concentration per unit leaf dry mass.

varied 4.5-fold ( $L_l$ ) to 19-fold ( $L_a$ ), leaf anatomical traits (leaf thickness,  $T_{leaf}$ ; LMA; and leaf density,  $\rho_{leaf}$ ) varied ~2-fold and LMA ranged from c. 41 to 100 g m<sup>-2</sup> (Table 1, Supporting Information: Table S3). *M. × giganteus* photosynthetic rates varied 6.2-fold for  $A_a$  and 8.1-fold for  $A_m$ , whereas the variations in stomatal conductance were 11-fold for  $g_{sa}$  and 13-fold for  $g_{sm}$ , respectively (Table 1). iWUE, nitrogen ( $N_a$  and  $N_m$ ) and phosphorus ( $P_a$  and  $P_m$ ) varied 2- to 3-fold across all genotypes (Table 1). Leaf traits also varied considerably among genotypes at each site and in each year (Supporting Information: Table S3).

In comparison, *M. × giganteus* showed a broader distribution of leaf traits than sorghum (Table 1 and Figure 1). Specifically, *M. × giganteus* showed higher LMA but lower photosynthesis,  $N_m$  and  $A_N$  compared to sorghum (Table 1). Although most of the leaf traits fell in the range of values reported in Glopnet, C<sub>4</sub> crops exhibited a lower mean LMA and higher mean photosynthesis, iWUE,  $N_m$  and  $A_N$  than the C<sub>3</sub> species represented in Glopnet. The mean  $P_a$ ,  $P_m$  and  $A_P$  in *M. × giganteus* were generally the same as those for Glopnet (Table 1). As a result, *M. × giganteus* and sorghum occupied a distinct niche in the global LES and tended to have high  $A_m$  and  $A_a$  at a given LMA or  $N_m$  (Figure 1).

Leaf traits in *M. × giganteus* also respond strongly to environmental drivers and stand age. In the 2019 season, plants produced larger and thinner leaves than in the 2018 season at the EF of the University of Illinois (Supporting Information: Table S3). The 2018 and 2019 plants also

differed in photosynthesis and nutrient content, with the 2018 plants showing lower  $A_m$  and higher stomatal conductance and nitrogen concentration. Genotypes at the MAFES of Mississippi State University showed smaller and thicker leaves with lower  $A_m$  and stomatal conductance than that at EF, perhaps because of greater precipitation and higher temperatures in Mississippi (Supporting Information: Table S3). However, no significant differences ( $p > 0.05$ ) were detected in  $A_a$  measured at the EF in different years or  $g_{sa}$  measured at different sites in 2019 (2019 IL vs. 2019 MS) (Supporting Information: Table S3). When using the same genotypes studied at two sites in both years, similar site and year effects on leaf traits were discovered (Supporting Information: Figures S1–S3). Genotypic variation, year/site effect and their interactions were found in LES traits (Supporting Information: Table S4).

### 3.2 | Correlations among leaf traits

Pearson's correlation analysis revealed broad relationships among leaf morphology, anatomy, photosynthesis and nutrient composition in *M. × giganteus* genotypes. Smaller and narrower leaves tended to be thicker, with higher LMA but lower photosynthetic rate and stomatal conductance (Figure 2, Supporting Information: Figure S4). Both  $A_a$  and  $A_m$  were negatively associated with  $T_{leaf}$  and LMA, and the

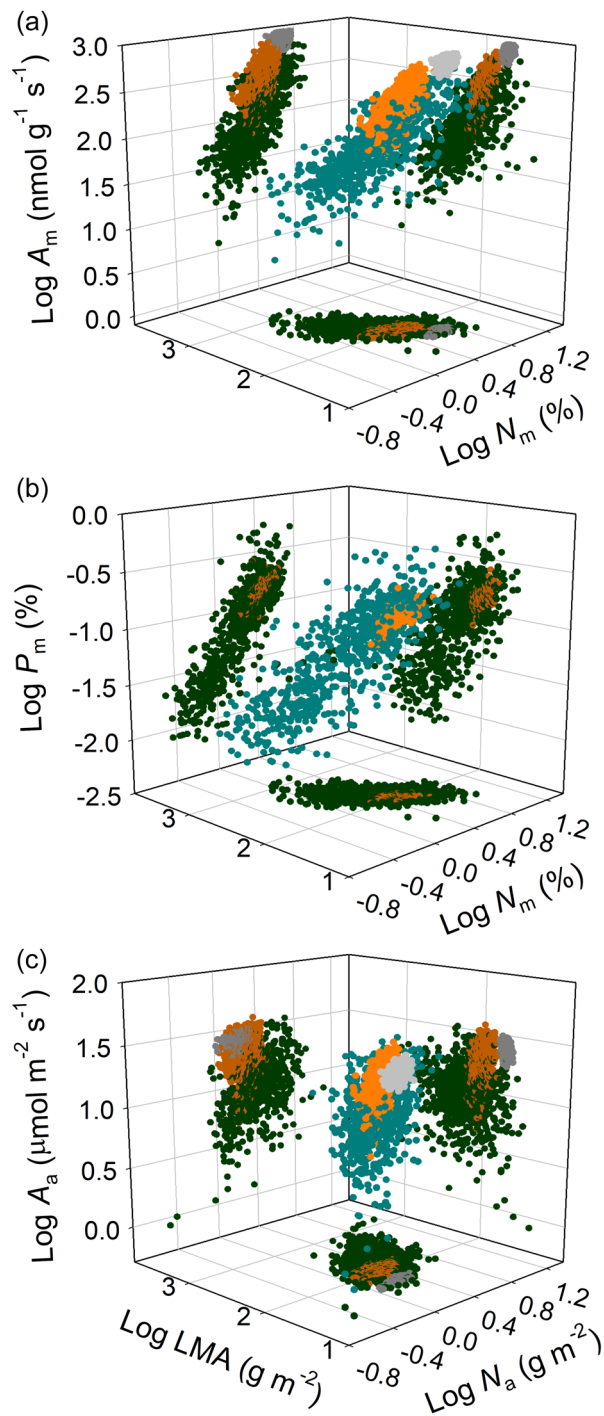


**FIGURE 1** Relationships among leaf economics spectrum traits in *Miscanthus* × *giganteus*, *Sorghum bicolour* and all species in the full Glopnet database. (a) Leaf maximum photosynthetic rate per unit dry mass ( $A_m$ ), leaf dry mass per area (LMA) and leaf nitrogen content per mass ( $N_m$ ). (b) Leaf phosphorus content per mass ( $P_m$ ), LMA and  $N_m$ . (c) Leaf maximum photosynthetic rate per unit area ( $A_a$ ), LMA and leaf nitrogen content per area ( $N_a$ ). *M. × giganteus* data are shown in orange points, *S. bicolour* data (Ferguson et al., 2021) are represented by grey points, and the Glopnet data (Wright et al., 2004) are shown in cyan points. The linear fits to *M. × giganteus* data and to the Glopnet database are given in Figure 4. Slopes and intercepts were estimated by standardized major axis regression and are provided in Table 3.

correlations were stronger when photosynthetic rate was expressed per unit leaf dry mass rather than per unit area (Figure 2, Supporting Information: Figure S4). There was a significant correlation between  $g_{sm}$  and LMA (Figure 2), but  $g_{sa}$  was not correlated with LMA (Supporting Information: Figure S4).  $N_m$  and  $P_m$  were negatively related to LMA but positively correlated with  $A_m$  (Figure 2).  $A_a$  was independent of area-based nutrient content, which scaled positively with LMA (Supporting Information: Figure S4). Notably,  $A_N$  and  $A_P$  increased with increasing  $A_a$  and  $A_m$  but decreasing  $T_{leaf}$  and LMA (Figure 2, Supporting Information: Figure S4). Chlorophyll fluorescence parameters were not correlated with leaf morphology, anatomy or nutrient content (Figure 2, Supporting Information: Figure S4). When individual sites and years were analyzed independently, similar patterns were observed, but the correlations among traits were less pronounced (Supporting Information: Figure S5). Although environmental conditions and stand age altered the absolute value of LES traits (Supporting Information: Figures S1–S3; Table S3), their correlations were largely consistent regardless of environment (Supporting Information: Figure S5).

### 3.3 | Comparison between triploids and tetraploids

Triploid and tetraploid *M. × giganteus* genotypes differed in most leaf traits (Table 2, Supporting Information: Table S5). Pooling all sites and years, tetraploids had thicker leaves with greater LMA and lower  $\rho_{leaf}$  than triploids (Table 2). Tetraploid leaves tended to have a lower  $A_m$  and  $iWUE$  but a higher  $g_{sa}$ ,  $C_i$ , chlorophyll fluorescence and  $N_a$  compared to those of triploids (Table 2). However, no significant differences in  $A_a$ ,  $g_{sm}$ ,  $N_m$  and  $P$  content were found between triploids and tetraploids (Table 2). We observed a similar difference in leaf traits between triploids and tetraploids when sites and years were analyzed independently (Supporting Information: Table S5).

Pooling all *M. × giganteus* data together,  $A_m$ ,  $N_m$  and  $P_m$  scaled negatively with LMA in both triploid and tetraploid genotypes (Figure 3a–c). Triploids showed a significantly lower intercept but a parallel slope to that of tetraploids in the correlation between  $A_m$  and LMA, indicating that at a given LMA, tetraploids have a higher photosynthetic rate (Figure 3a). For  $N_m$  versus LMA, the differences in both slope and intercept between triploid and tetraploid genotypes were substantial (Figure 3b). The significant difference in slope ( $p < 0.005$ ) was detected in  $P_m$  versus LMA between triploids and tetraploids (Figure 3c). Positive relationships between  $A_m$  and  $N_m$ , between  $P_m$  and  $N_m$ , and between  $A_m$  and  $P_m$  were observed in both triploid and tetraploid genotypes and no significant differences ( $p > 0.05$ ) in slopes or intercepts in any relationships were observed (Figure 3d–f). The bivariate relationships remained robust in triploids at different sites/years (Supporting Information: Figures S6–S8). However, the small sample size for leaf functional traits in tetraploids at each site or in each year reduced the statistical power of the bivariate relationships (Supporting Information: Figures S6–S8).

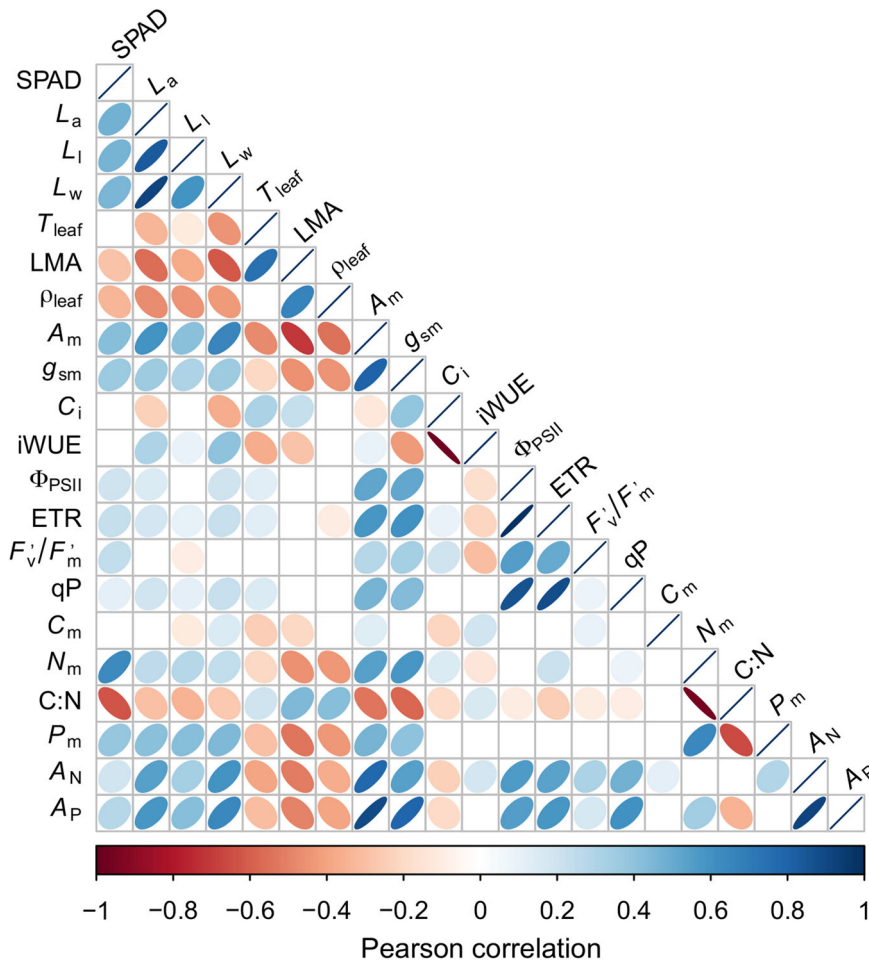


**FIGURE 2** Pearson's correlations of leaf traits (mass basis) using the full data set from *Miscanthus × giganteus*. The ellipses correspond to the significant correlations ( $p < 0.05$ ) with colours from blue (positive correlation) to red (negative correlation) indicating strength of correlation. Trait abbreviations and units are provided in Supporting Information: Table S2. [Color figure can be viewed at [wileyonlinelibrary.com](http://wileyonlinelibrary.com)]

### 3.4 | Comparison between *M. × giganteus* and the global LES

Although the bivariate LES trait correlation patterns in *M. × giganteus* were generally similar with the relationships observed across natural species in the Glopnet database, *M. × giganteus* showed a distinguishable niche in the global LES (Figure 1). Specifically, *M. × giganteus* had a lower  $r^2$  of significant trait–trait relationships ( $p < 0.0001$ ) than those in the species in Glopnet, suggesting less constraint in functional trait trade-offs (Figure 4). A summary of the results of all SMA analyses of *M. × giganteus* is given in Table 3. The slopes and intercepts of the major bivariate correlations of the leaf traits in *M. × giganteus* genotypes were significantly different from the Glopnet database (Table 3). For instance, the correlation between  $A_m$  and LMA in *M. × giganteus* exhibited a significantly higher intercept but lower slope than the Glopnet species (Figure 4). The SMA analysis also revealed that there were significant differences in the slopes and intercepts of bivariate LES trait relationships between triploids and the Glopnet database and between tetraploids and the Glopnet database (Table 4; Supporting Information: Figures S9 and S10). Moreover, bivariate relationships among LMA,  $A_m$ ,  $N_m$  and  $P_m$  of studied *M. × giganteus* at different sites/years and the species in Glopnet differed significantly in terms of their slopes and intercepts (Supporting Information: Table S6).

## 4 | DISCUSSION

*M. × giganteus* has become an emerging and promising  $C_4$  feedstock for bioenergy and bioproducts owing to its broad adaptation, high biomass productivity and low nutrient input requirement (Clifton-Brown et al., 2017; Heaton et al., 2008; Lewandowski et al., 2000). Greater understanding of leaf functional traits and trait relationships will help to guide efforts to further improve resource use efficiency and productivity in *M. × giganteus*. Here, we constructed a large database of leaf functional traits including 585 observations for 239 *M. × giganteus* genotypes in two common gardens in 2018 and 2019 (Supporting Information: Table S1). We compared leaf functional traits of *M. × giganteus* with published values from sorghum and the global LES. Our results reveal substantial genotypic trait variation in *M. × giganteus* and highlight significant differences in leaf trait and trait relationships between triploids and tetraploids. In comparison with the global data set of species, the  $C_4$  species, *M. × giganteus* and sorghum, displayed higher photosynthetic rate, greater water and nitrogen use efficiency and deviation in LES trait relationships.

The global LES was developed with data from species in natural ecosystems and originally did not include crops grown in agricultural environments. More recently, studies demonstrated that the

**TABLE 2** Comparison of leaf functional traits between triploid and tetraploid *Miscanthus* × *giganteus* genotypes

Trait	Triploid Range	Mean	Tetraploid Range	Mean	p Value
$T_{\text{leaf}}$	129.2–226.4	166.2	132.4–239.9	190.7	<0.001
LMA	41.0–91.9	63.2	46.0–90.2	69.4	<0.001
$\rho_{\text{leaf}}$	0.29–0.57	0.38	0.26–0.46	0.36	0.001
$A_a$	7.8–41.0	24.2	7.1–36.5	24.9	0.32
$A_m$	99.5–733.8	398.0	94.9–758.2	372.1	0.07
$g_{\text{sa}}$	0.048–0.436	0.184	0.046–0.507	0.211	<0.001
$g_{\text{sm}}$	0.53–6.50	3.00	0.62–6.85	3.12	0.35
$C_i$	77.6–267.7	156.8	30.9–256.3	177.1	<0.001
iWUE	72.6–196.0	141.6	82.4–227.8	127.7	<0.001
$\Phi_{\text{PSII}}$	0.067–0.327	0.209	0.093–0.313	0.231	<0.001
ETR	52.0–247.4	164.8	72.1–243.2	181.6	<0.001
$F_v'/F_m'$	0.27–0.58	0.43	0.30–0.59	0.44	0.017
qP	0.20–0.69	0.49	0.27–0.67	0.52	0.001
$N_a$	0.83–2.01	1.42	0.82–2.41	1.53	0.001
$N_m$	1.35–3.09	2.28	1.16–3.13	2.23	0.29
$P_a$	0.071–0.151	0.107	0.074–0.157	0.108	0.66
$P_m$	0.096–0.255	0.172	0.087–0.293	0.166	0.22

Note: Means between triploid and tetraploid genotypes were compared with one-way analysis of variance followed by Tukey test. There was no significant differences between triploid and tetraploid genotypes in other leaf traits not shown in this table. Trait abbreviations and units are provided in Supporting Information: Table S2.

Abbreviations:  $C_i$ , intercellular  $\text{CO}_2$  concentration; ETR, electron transport rate;  $F_v'/F_m'$ , photosystem II maximum efficiency; LMA, leaf mass per unit area;  $\Phi_{\text{PSII}}$ , quantum yield of photosystem II; qP, coefficient of photochemical quenching.

relationships among LES traits in crop species in agricultural systems were similar to the universal LES worldwide (Hayes et al., 2019; Martin et al., 2017, 2018; Xiong & Flexas, 2018). These previous analyses focused on  $C_3$  crops such as rice, wheat and soybean. To date, the only  $C_4$  species studied for LES is maize, where very limited observations were included (Martin et al., 2018). In this study, we compared LES trait relationships between two  $C_4$  bioenergy species, *M. × giganteus* and sorghum, and the Glopnet database (Figure 1). We found a similar trend in LES trait relationships between the two data sets, suggesting principles of leaf design behind trait–trait associations in  $C_4$  species have similarities with those in  $C_3$  species. There was greater variation within the 239 *M. × giganteus* genotypes than within 869 sorghum genotypes (Figure 1), despite the representation of four major races from three continents in the sorghum collection (Valluru et al., 2019). This perhaps reflects less selection in *M. × giganteus*. However, it should be noted that sorghum leaf-level gas exchange was taken from excised leaves in laboratory conditions which were less variable than measurements conditions in the field (Ferguson et al., 2021). In the global LES,  $A_m$ ,  $N_m$  and  $P_m$  negatively correlated with LMA, indicating “fast-slow” resource strategies. This is particularly true for  $C_3$  species, where species with higher LMA

tend to have thicker leaves and greater tissue density resulting in more self-shading of chloroplasts, greater  $\text{CO}_2$  diffusive resistance and longer  $\text{CO}_2$  diffusion pathways from stomata to chloroplasts, resulting in lower photosynthetic rates (Hikosaka, 2004; Niinemets, 1999; Onoda et al., 2017; Poorter et al., 2009). In addition, leaves with higher LMA tend to have lower  $N_m$  and  $P_m$ , and lower  $A_N$  and  $A_P$ , which act as a constraint on plant growth (Hikosaka, 2004; Reich & Schoettle, 1988). The robust leaf trait relationships in *M. × giganteus* indicate the important role of leaf anatomy in determining leaf function in  $C_4$  species (Figure 2, Supporting Information: Figure S4). The key question is why is photosynthesis tightly associated with LMA in  $C_4$  species? In *M. × giganteus*,  $T_{\text{leaf}}$  and  $\rho_{\text{leaf}}$  increased with increasing LMA (Figure 2), suggesting that increased LMA resulted in increased mesophyll thickness, bundle sheath size and  $\text{CO}_2$  diffusion pathways within leaf. However,  $\text{CO}_2$  concentration and diffusion within the leaf are unlikely to be a major limitation to photosynthesis in  $C_4$  species because of the  $\text{CO}_2$ -concentrating mechanism in bundle sheath cells (Hatch, 1987; Leakey et al., 2006; Sage, 2004). Thicker leaves and larger bundle sheath size resulting from high LMA may contribute to non-uniform light distribution within a leaf. The presence of shade on the lower side of bundle sheath cells strongly



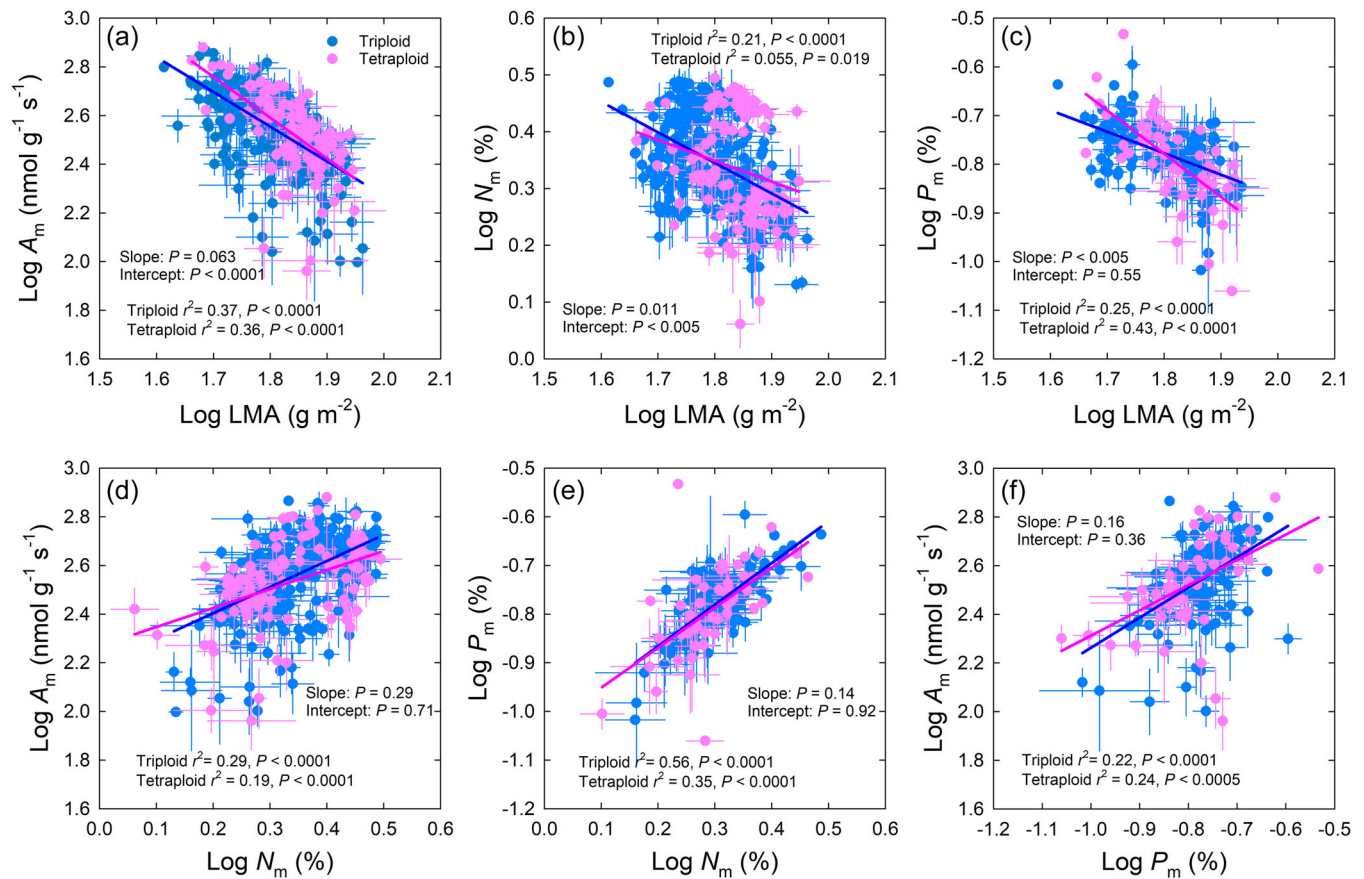


**FIGURE 3** Relationships among leaf dry mass per area (LMA),  $A_m$ ,  $N_m$  and  $P_m$  in triploid and tetraploid genotypes of *Miscanthus x giganteus*. (a) Leaf maximum photosynthetic rate per unit dry mass ( $A_m$ ) versus LMA. (b) Leaf nitrogen content per mass ( $N_m$ ) versus LMA. (c) Leaf phosphorus content per mass ( $P_m$ ) versus LMA. (d)  $A_m$  versus  $N_m$ . (e)  $A_m$  versus  $P_m$ . (f)  $N_m$  versus  $P_m$ . Differences in slopes and intercepts were compared between triploid and tetraploid genotype by standardized major axis. Error bars show SEs. All values were  $\log_{10}$ -transformed. [Color figure can be viewed at [wileyonlinelibrary.com](http://wileyonlinelibrary.com)]

reduces Rubisco content and activity, ATP production and ribulose-1,5-bisphosphate (RuBP) regeneration capacity (Bellasio & Lundgren, 2016; Tazoe et al., 2006), decreasing photosynthesis. Although Rubisco content per unit leaf area was not significantly associated with LMA (Onoda et al., 2017), the negative correlation between LMA and photosynthesis normalized by Rubisco was amongst the most stable relationships (Poorter et al., 2014). This further supports that the leaf internal environment, metabolic processes and enzyme activities underpin the leaf structural and physiological tradeoffs.

Significant changes in the slope and intercept of LES trait relationships were detected between *M. x giganteus* and the Glopnet database (Table 3, Supporting Information: Table S6). At a given LMA, *M. x giganteus* showed a higher  $A_m$  than most of the Glopnet species without greater increases in  $N_m$  and  $P_m$  (Figures 1 and 4), indicating higher photosynthetic efficiency in the  $C_4$  species. *M. x giganteus* genotypes also tended to have a higher  $A_m$  at a given  $N_m$  or  $P_m$  when compared to the Glopnet species, in agreement with the observations of higher  $A_N$  and  $A_P$  in *M. x giganteus* (Table 1). Notably, *M. x giganteus* genotypes have intermediate values for LMA,  $A_a$ ,  $A_m$  and  $N_m$  among other studied  $C_4$  species. For example, sorghum exhibited a lower mean LMA but high mean photosynthesis, iWUE,  $N_m$  and  $A_N$  than the

*M. x giganteus* genotypes presented here (Table 1; Figure 1) (Ferguson et al., 2021). In other studies, the lowest reported  $A_a$ ,  $A_m$  and  $N_m$  values for five genotypes of sorghum were 44.3  $\mu\text{mol m}^{-2} \text{s}^{-1}$ , 1426.7  $\text{nmol g}^{-1} \text{s}^{-1}$  and 3.76% (Li et al., 2019, 2021), beyond the highest values of 41.0  $\mu\text{mol m}^{-2} \text{s}^{-1}$ , 758.2  $\text{nmol g}^{-1} \text{s}^{-1}$  and 3.19% in the *M. x giganteus* database. Concerning LMA, the highest value for sorghum was 35.3  $\text{g m}^{-2}$ , which is much lower than the lowest values of 41.0  $\text{g m}^{-2}$  in *M. x giganteus*. However, switchgrass (*Panicum virgatum*; three genotypes) had a similar mean LMA value with *M. x giganteus* (67.4 vs. 67.1  $\text{g m}^{-2}$ ), but displayed overall higher mean values for  $A_a$  (30.6 vs. 23.7  $\mu\text{mol m}^{-2} \text{s}^{-1}$ ),  $A_m$  (456.6 vs. 369.8  $\text{nmol g}^{-1} \text{s}^{-1}$ ), and  $N_m$  (3.37 vs. 2.20%) (Li et al., 2019, 2022). A recent study also revealed broad variation in leaf morphology across switchgrass genotypes in common garden experiments (Lovell et al., 2021). These results suggest that  $C_4$  species may differ in their trait-trait relationships and resource use strategies reinforcing the importance of trait variation in  $C_4$  species in shifting the cross-species LES worldwide. We also observed the bivariate relationships of both triploids and tetraploids differ significantly from the global data set (Table 4; Supporting Information: Figures S9 and S10). It should be noted that a few pentaploid and hexaploid genotypes were measured

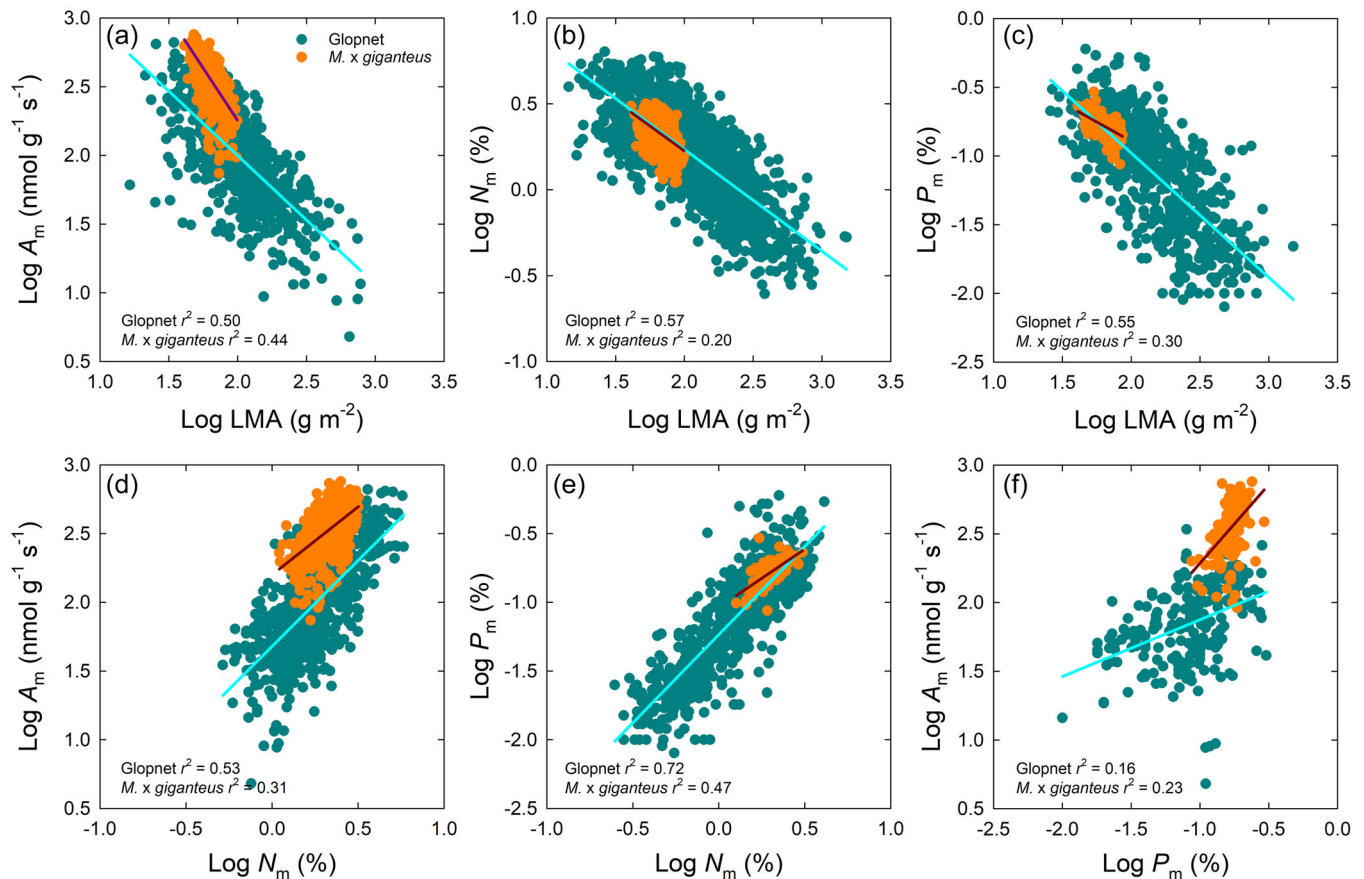


**FIGURE 4** Relationships among leaf economics spectrum traits in *Miscanthus × giganteus* compared with the global pattern using the Glopnet database. (a) Leaf maximum photosynthetic rate per unit dry mass ( $A_m$ ) versus leaf dry mass per area (LMA). (b) Leaf nitrogen content per mass ( $N_m$ ) versus LMA. (c) Leaf phosphorus content per mass ( $P_m$ ) versus LMA. (d)  $A_m$  versus  $N_m$ . (e)  $A_m$  versus  $P_m$ . (f)  $N_m$  versus  $P_m$ . In all case, regressions to all *M. × giganteus* data and to the total Glopnet database were statistically significant at  $p < 0.0001$ . [Color figure can be viewed at [wileyonlinelibrary.com](http://wileyonlinelibrary.com)]

**TABLE 3** Mass basis of bivariate relationships in *Miscanthus × giganteus* and comparison of the bivariate relationships between *M. × giganteus* and Glopnet

	Log LMA		Log $N_m$		Log $P_m$		Log $A_m$	
	Slope	Intercept	Slope	Intercept	Slope	Intercept	Slope	Intercept
Log LMA			-1.30 (-1.21, -1.40)	1.85 (1.81, 1.90)	-1.02 (-0.90, -1.16)	1.36 (1.26, 1.46)	-2.30 (-2.16, -2.45)	5.53 (5.40, 5.65)
Log $N_m$	<b>&lt;0.001</b>	<b>&lt;0.001</b>			1.23 (1.11, 1.38)	-1.23 (-1.25, -1.21)	1.77 (1.66, 1.90)	1.95 (1.93, 1.98)
Log $P_m$	0.01	<b>&lt;0.001</b>	<b>&lt;0.001</b>	0.012			2.41 (2.10, 2.75)	3.71 (3.60, 3.82)
Log $A_m$	<b>&lt;0.001</b>	<b>&lt;0.001</b>	0.44	<b>&lt;0.001</b>	<b>&lt;0.001</b>	<b>&lt;0.001</b>		

Note: The *M. × giganteus* data was analyzed by standardized major axis regression analysis. Slopes and intercepts with 95% confidence intervals are given in the upper-right section of the matrix (x variable in column 1, y variable in row 1). The differences in slopes and intercepts between *M. × giganteus* and Glopnet are given in the lower-left section of the matrix. Significant differences ( $p < 0.05$ ) are shown in boldface. Trait abbreviations and units are provided in Supporting Information: Table S2.

in the present study (Supporting Information: Table S1). Both pentaploids and hexaploids show lower average values of  $A_a$ ,  $A_m$  and  $N_m$  but higher mean value of LMA than triploids and tetraploids. However, we cannot completely identify the leaf trait differences from triploids to hexaploids and assess the contributions of

pentaploids and hexaploids to global LES due to the limited number of genotypes sampled.

Leaf functional traits such as LMA and photosynthesis show plasticity in response to different conditions such as temperature, light, water and nutrient availability in natural environments (Poorter

TABLE 4 Comparison of the bivariate relationships between triploid or tetraploid genotypes of *Miscanthus × giganteus* and Glopnet

Log LMA	Triplet Tetraploid	Log LMA		Log N <sub>m</sub>		Log P <sub>m</sub>		Log A <sub>m</sub>	
		Slope	Intercept	Slope	Intercept	Slope	Intercept	Slope	Intercept
Log N <sub>m</sub>	Triploid	<0.001	<0.001	-1.18 (-1.06, 1.31)	1.79 (1.75, 1.83)	-0.88 (-0.75, 1.03)	1.35 (1.25, 1.45)	-2.35 (-2.14, 2.58)	5.23 (5.11, 5.35)
	Tetraploid	<0.001	0.001	-1.57 (-1.29, 1.90)	1.79 (1.74, 1.84)	-1.35 (-1.09, 1.68)	1.43 (1.32, 1.54)	-2.80 (-2.39, 3.28)	5.10 (4.97, 5.23)
Log P <sub>m</sub>	Triploid	<0.001	<0.001	<0.001	<0.05	1.14 (1.01, 1.29)	-1.23 (-1.25, 1.21)	2.00 (1.81, 2.21)	1.95 (1.91, 1.98)
	Tetraploid	0.35	<0.001	0.48	0.13	1.39 (1.10, 1.75)	-1.23 (-1.26, 1.20)	1.79 (1.49, 2.13)	1.95 (1.91, 2.00)
Log A <sub>m</sub>	Triploid	<0.001	<0.001	0.008	<0.001	<0.001	<0.001	2.63 (2.24, 3.09)	3.64 (3.52, 3.75)
	Tetraploid	<0.001	<0.001	0.67	<0.001	<0.001	<0.001	2.13 (1.66, 2.74)	3.45 (3.34, 3.57)

Note: The data set of triploid and tetraploid genotypes was analyzed by standardized major axis (SMA) regression. SMA slopes and intercepts with 95% confidence intervals are given in the upper-right section of the matrix (x variable in column 1, y variable in row 1). The differences in slopes and intercepts between triploid genotypes (first row of each trait) and Glopnet and between tetraploid genotypes (second row of each trait) and Glopnet are given in the lower-left section of the matrix. Significant differences ( $p < 0.05$ ) are shown in boldface. Trait abbreviations and units are provided in Supporting Information: Table S2.

et al., 2009). Our results also showed significant site/year effects on leaf functional traits in *M. × giganteus* genotypes (Supporting Information: Table S4; Figures S1–S3) and most of the variance in phosphorus content was associated with environment, not genotype or genotype × environment interaction (Supporting Information: Table S4). Previous studies of leaf functional traits also extrapolated that phenotypic plasticity was the dominant source of within-species trait variability in *Eucalyptus camaldulensis* and *Quercus ilex* (Asao et al., 2020; Niinemets, 2015; Valladares et al., 2002), although genotypic variation explained significant variation in leaf functional traits in nine switchgrass genotypes (Aspinwall et al., 2013). Differences in plant/leaf age and sampling time can be another source of within-species trait variation in multiple species or the Glopnet database (Mason et al., 2013; McKown et al., 2013; Niinemets, 2015; Niinemets et al., 2005). In our study, all genotypes were planted on the same date and all leaves used for the measurements had similar age at each site and in each year, minimizing the effect of plant/leaf age on leaf traits. Still, the site and year in which measurements were made had a significant effect on LES traits. There were explicit differences in leaf functional traits and trait relationships between ploidy levels (Figure 3; Table 2; Supporting Information: Table S5). However, we also found significant variation within both triploids and tetraploids, suggesting the contribution of ploidy levels to overall species trait variation was limited. Nevertheless, polyploidization-induced genotypic variation in leaf functional traits may have practical implications for improving photosynthetic efficiency and crop productivity.

In conclusion, our study is the first to explicitly quantify the contributions of genotypic trait variation and ploidy levels in *C<sub>4</sub>* species in agricultural systems to global LES. The large trait variation across genotypes of *M. × giganteus* and correlations between nutrient content and photosynthetic efficiency provide an opportunity to improve photosynthetic and resource use efficiency and crop productivity. We argue that genotypic trait variation and ploidy levels in more *C<sub>4</sub>* species may obscure or alter the general broad LES trait relationships and therefore needs more attention in the global trait databases. Future efforts to investigate additional *C<sub>4</sub>* species in both natural and agricultural systems are required to improve data coverage in the global database and gain further insight into universal relationships between leaf traits and resource use strategy.

#### ACKNOWLEDGEMENTS

We thank Hannah Demler and Congying Wu for lab and field assistance. We also thank Drs. Jiayang Xie and Zhihai Zhang for statistical analyses and Drs. Christopher M. Montes and Anthony Digrado for helpful discussions. This work was funded by the DOE Center for Advanced Bioenergy and Bioproducts Innovation (U.S. Department of Energy, Office of Science, Office of Biological and Environmental Research under Award Number DE-SC0018420). Any opinions, findings, and conclusions or recommendations expressed in this publication are those of the author(s) and do not necessarily reflect the views of the U.S.

Department of Energy (DOE) or the U.S. Department of Agriculture (USDA). Mention of trade names or commercial products in this publication is solely for the purpose of providing specific information and does not imply recommendation or endorsement by the USDA. USDA is an equal opportunity provider and employer. This study was funded by U.S. Department of Energy, Grant/Award Number: DE-SC0018420.

## CONFLICT OF INTEREST

The authors declare no conflict of interest.

## DATA AVAILABILITY STATEMENT

The data that support the findings of this study are available on request from the corresponding author.

## ORCID

Shuai Li  <http://orcid.org/0000-0003-2545-7763>

Erik J. Sacks  <http://orcid.org/0000-0001-7537-4558>

John N. Ferguson  <http://orcid.org/0000-0003-3603-9997>

Andrew D. B. Leakey  <http://orcid.org/0000-0001-6251-024X>

Elizabeth A. Ainsworth  <http://orcid.org/0000-0002-3199-8999>

## REFERENCES

- Albert, C.H., Thuiller, W., Yoccoz, N.G., Soudant, A., Boucher, F., Saccone, P. et al. (2010) Intraspecific functional variability: extent, structure and source of variation. *Journal of Ecology*, 98, 604–613.
- Anderegg, L.D.L., Berner, L.T., Badgley, G., Sethi, M.L., Law, B.E. & HilleRisLambers, J. (2018) Within-species patterns challenge our understanding of the leaf economics spectrum. *Ecology Letters*, 21, 734–744.
- Asao, S., Hayes, L., Aspinwall, M.J., Rymer, P.D., Blackman, C., Bryant, C.J. et al. (2020) Leaf trait variation is similar among genotypes of *Eucalyptus camaldulensis* from differing climates and arise in plastic responses to the seasons rather than water availability. *New Phytologist*, 227, 780–793.
- Aspinwall, M.J., Lowry, D.B., Taylor, S.H., Juenger, T.E., Hawkes, C.V., Johnson, M.V. et al. (2013) Genotypic variation in traits linked to climate and aboveground productivity in a widespread C<sub>4</sub> grass: evidence for a functional trait syndrome. *New Phytologist*, 199, 966–980.
- Bagheri, M. & Mansouri, H. (2015) Effect of induced polyploidy on some biochemical parameters in *Cannabis sativa* L. *Applied Biochemistry and Biotechnology*, 175, 2366–2375.
- Baker, R.L., Yarkhunova, Y., Vidal, K., Ewers, B.E. & Weing, C. (2017) Polyploidy and the relationship between leaf structure and function: implications for correlated evolution of anatomy, morphology, and physiology in Brassica. *BMC Plant Biology*, 17, 3.
- Bellasio, C. & Lundgren, M.R. (2016) Anatomical constraints to C<sub>4</sub> evolution: light harvesting capacity in the bundle sheath. *New Phytologist*, 212, 485–496.
- Blonder, B., Vasseur, F., Violle, C., Shipley, B., Enquist, B.J. & Vile, D. (2015) Testing models for the leaf economics spectrum with leaf and whole-plant traits in *Arabidopsis thaliana*. *AoB Plants*, 7, plv049.
- Blonder, B., Violle, C. & Enquist, B.J. (2013) Assessing the causes and scales of the leaf economics spectrum using venation network in *Populus tremuloides*. *Journal of Ecology*, 101, 981–989.
- Chae, W.B. (2012). *Cytogenetics and genome structure in genus Miscanthus, a potential source of bioenergy feedstocks*. PhD thesis, University of Illinois at Urbana-Champaign, IL, USA.
- Chao, D.-Y., Dilkes, B., Luo, H., Douglas, A., Yakubova, E., Lahner, B. et al. (2013) Polyploids exhibit higher potassium uptake and salinity tolerance in *Arabidopsis*. *Science*, 341, 658–659.
- Clark, L.V., Jin, X., Petersen, K.K., Anzoua, K.G., Bagmet, L., Chebukin, P. et al. (2019) Population structure of *Miscanthus sacchariflorus* reveals two major polyploidization events, tetraploid-mediated unidirectional introgression from diploid *M. sinensis*, and diversity centred around the Yellow Sea. *Annals of Botany*, 124, 731–748.
- Clark, L.V., Stewart, J.R., Nishiwaki, A., Toma, Y., Kjeldsen, J.B., Jørgensen, U. et al. (2015) Genetic structure of *Miscanthus sinensis* and *Miscanthus sacchariflorus* in Japan indicates a gradient of bidirectional but asymmetric introgression. *Journal of Experimental Botany*, 66, 4213–4225.
- Clifton-Brown, J., Hastings, A., Mos, M., Mccalmon, J.P., Ashman, C., Awty-Carroll, D. et al. (2017) Progress in upscaling *Miscanthus* biomass production for the European bio-economy with seed-based hybrids. *Global Change Biology Bioenergy*, 9, 6–17.
- Dong, H., Green, S.V., Nishiwaki, A., Yamada, T., Stewart, J.R., Deuter, M. et al. (2019) Winter hardiness of *Miscanthus* (l): overwintering ability and yield of new *Miscanthus* × *giganteus* genotypes in Illinois and Arkansas. *Global Change Biology Bioenergy*, 11, 691–705.
- Ehleringer, J.R., Cerling, T.E. & Helliker, B.R. (1997) C<sub>4</sub> photosynthesis, atmospheric CO<sub>2</sub>, and climate. *Oecologia*, 112, 285–299.
- Ehleringer, J.R. & Monson, R.K. (1993) Evolutionary and ecological aspects of photosynthetic pathway variation. *Annual Review of Ecology and Systematics*, 24, 411–439.
- Ferguson, J.N., Fernandes, S.B., Monier, B., Miller, N.D., Allen, D., Dmitrieva, A. et al. (2021) Machine learning-enabled phenotyping for GWAS and TWAS of WUE traits in 869 field-grown sorghum. *Plant Physiology*, 187, 1481–1500.
- Głowacka, K., Clark, L.V., Adhikari, S., Peng, J., Stewart, J.R., Nishiwaki, A. et al. (2015) Genetic variation in *Miscanthus* × *giganteus* and the importance of estimating genetic distance threshold for differentiating clones. *Global Change Biology Bioenergy*, 7, 386–404.
- Hao, G.-Y., Lucero, M.E., Sanderson, S.C., Zacharias, E.H. & Holbrook, N.M. (2013) Polyploidy enhances the occupation of heterogeneous environments through hydraulic related trade-offs in *Atriplex canescens* (Chenopodiaceae). *New Phytologist*, 197, 970–978.
- Hatch, M.D. (1987) C<sub>4</sub> photosynthesis: a unique blend of modified biochemistry, anatomy and ultrastructure. *Biochimica et Biophysica Acta*, 895, 81–106.
- Hayes, F.J., Buchanan, S.W., Coleman, B., Gordon, A.M., Reich, P.B., Thevathasan, N.V. et al. (2019) Interspecific variation in soy across the leaf economics spectrum. *Annals of Botany*, 123, 107–120.
- Heaton, E.A., Dohleman, F.G. & Long, S.P. (2008) Meeting US biofuel with less land: the potential of *Miscanthus*. *Global Change Biology*, 14, 2000–2012.
- Hikosaka, K. (2004) Interspecific difference in the photosynthesis-nitrogen relationship: patterns, physiological causes, and ecological importance. *Journal of Plant Research*, 117, 481–497.
- Hodkinson, T.R., Chase, M.W., Takahashi, C., Leitch, I.J., Bennet, M.D. & Renvoize, S.A. (2002) The use of DNA sequencing (ITS and *TRNL-F*), AFLP, and fluorescent in situ hybridization to study allopolyploid *Miscanthus* (Poaceae). *American Journal of Botany*, 89, 279–286.
- Hodkinson, T.R. & Renvoize, S.A. (2001) Nomenclature of *Miscanthus* × *giganteus* (poaceae). *Kew Bulletin*, 56, 759–760.
- Leakey, A.D.B., Ferguson, J.N., Pignon, C.P., Wu, A., Jin, Z., Hammer, G.L. et al. (2019) Water use efficiency as a constraint and target for improving the resilience and productivity of C<sub>3</sub> and C<sub>4</sub> crops. *Annual review of plant biology*, 70, 781–808.
- Leakey, A.D.B., Uribelarra, M., Ainsworth, E.A., Naidu, S.L., Rogers, A., Ort, D.R. et al. (2006) Photosynthesis, productivity, and yield of

- maize are not affected by open-air elevation of CO<sub>2</sub> concentration in the absence of drought. *Plant Physiology*, 140, 779–790.
- Lewandowski, I., Clifton-Brown, J.C., Scurlock, J.M.O. & Huisman, W. (2000) *Miscanthus*: European experience with a novel energy crop. *Biomass and Bioenergy*, 19, 209–227.
- Li, S., Courbet, G., Ourry, A. & Ainsworth, E.A. (2019) Elevated ozone concentration reduces photosynthetic carbon gain but does not alter leaf structural traits, nutrient composition or biomass in switchgrass. *Plants*, 8, 85.
- Li, S., Moller, C.A., Mitchell, N.G., Lee, D. & Ainsworth, E.A. (2021) Bioenergy sorghum maintains photosynthetic capacity in elevated ozone concentrations. *Plant, Cell & Environment*, 44, 729–746.
- Li, S., Moller, C.A., Mitchell, N.G., Lee, D., Sacks, E.J. & Ainsworth, E.A. (2022) Testing unified theories for ozone response in C<sub>4</sub> species. *Global Change Biology*, 28, 3379–3393.
- Lovell, J.T., MacQueen, A.H., Mamidi, S., Bonnette, J., Jenkins, J., Napier, J.D. et al. (2021) Genomic mechanisms of climate adaptation in polyploidy bioenergy switchgrass. *Nature*, 590, 438–444.
- Martin, A.R., Hale, C.E., Cerabolini, B.E.L., Cornelissen, J.H.C., Craine, J., Gough, W.A. et al. (2018) Inter- and intraspecific variation in leaf economics traits in wheat and maize. *AoB Plants*, 10, ply006.
- Martin, A.R., Rapidel, B., Rounsard, O., Van den Meersche, K., de Melo Virginio Filho, E., Barrios, M. et al. (2017) Intraspecific trait variation across multiple scales: the leaf economics spectrum in coffee. *Functional Ecology*, 31, 604–612.
- Mason, C.M., McGaughey, S.E. & Donovan, L.A. (2013) Ontogeny strongly and differentially alters leaf economic and other key traits in three diverse *Helianthus* species. *Journal of Experimental Botany*, 64, 4089–4099.
- Masterson, J. (1994) Stomatal size in fossil plants: evidence for polyploidy in majority of angiosperms. *Science*, 264, 421–424.
- McKown, A.D., Guy, R.D., Azam, M.S., Drewes, E.C. & Quamme, L.K. (2013) Seasonality and phenology alter functional leaf traits. *Oecologia*, 172, 653–665.
- Montes, C.M., Demler, H.J., Li, S., Martin, D.G. & Ainsworth, E.A. (2022) Approaches to investigate crop response to ozone pollution: from O<sub>3</sub>-FACE to satellite-enabled modeling. *Plant Journal*, 109, 432–446.
- Niinemets, Ü. (1999) Components of leaf dry mass per area-thickness and density-alter leaf photosynthetic capacity in reverse directions in woody plants. *New Phytologist*, 144, 35–47.
- Niinemets, Ü. (2015) Is there a species spectrum within the world-wide leaf economics spectrum? Major variations in leaf functional traits in the Mediterranean sclerophyll *Quercus ilex*. *New Phytologist*, 205, 79–96.
- Niinemets, Ü., Cescatti, A., Rodeghiero, M. & Tosens, T. (2005) Leaf internal diffusion conductance limits photosynthesis more strongly in older leaves of Mediterranean evergreen broad-leaved species. *Plant, Cell & Environment*, 28, 1552–1566.
- Onoda, Y., Wright, I.J., Evans, J.R., Hikosaka, K., Kitajima, K., Niinemets, Ü. et al. (2017) Physiological and structural tradeoffs underlying the leaf economics spectrum. *New Phytologist*, 214, 1447–1463.
- Poorter, H., Lambers, H. & Evans, J.R. (2014) Trait correlation networks: a whole-plant perspective on the recently criticized leaf economic spectrum. *New Phytologist*, 201, 378–382.
- Poorter, H., Niinemets, Ü., Poorter, L., Wright, I.J. & Villar, R. (2009) Causes and consequences of variation in leaf mass per area (LMA): a meta-analysis. *New Phytologist*, 182, 565–588.
- Quinn, L.D., Allen, D.J. & Stewart, J.R. (2010) Invasiveness potential of *Miscanthus sinensis*: implications for bioenergy production in the United States. *Global Change Biology*, 2, 310–320.
- Ranum, P., Peña-Rosas, J.P. & Garcia-Casal, M.N. (2014) Global maize production, utilization, and consumption. *Annals of the New York Academy of Sciences*, 1312, 105–112.
- Rayburn, A.L., Crawford, J., Rayburn, C.M. & Juvik, J.A. (2009) Genome size of three *Miscanthus* species. *Plant Molecular Biology Reporter*, 27, 184–188.
- Reich, P.B. (2014) The world-wide “fast-slow” plant economics spectrum: a traits manifesto. *Journal of Ecology*, 102, 275–301.
- Reich, P.B. & Schoettle, A.W. (1988) Role of phosphorus and nitrogen in photosynthetic and whole plant carbon gain and nutrient use efficiency in eastern white pine. *Oecologia*, 77, 25–33.
- Reich, P.B., Walters, M.B. & Ellsworth, D.S. (1997) From tropics to tundra: global convergence in plant functioning. *Proceedings of the National Academy of Sciences, USA*, 94, 13730–13734.
- Rooney, W.L., Blumenthal, J., Bean, B., & Mullet, J.E. (2007) Designing sorghum as a dedicated bioenergy feedstock. *Biofuels, Bioproducts & Biorefining*, 1, 147–157.
- Sage, R.F. (2004) The evolution of C<sub>4</sub> photosynthesis. *New Phytologist*, 161, 341–370.
- Sage, R.F., Li, M.R. & Monson, R.K. (1999) The taxonomic distribution of C<sub>4</sub> photosynthesis. In: Sage, R.F. & Monson, R.K. (Eds.), *C<sub>4</sub> plant biology*. Academic Press, pp. 551–584.
- Soil Survey Staff. 2015. *Natural Resources Conservation Service, United States Department of Agriculture. Official soil series descriptions*. Available at [https://www.nrcs.usda.gov/wps/portal/nrcs/detail/soils/scientists/?cid=nrcs142p2\\_053587](https://www.nrcs.usda.gov/wps/portal/nrcs/detail/soils/scientists/?cid=nrcs142p2_053587)
- Soltis, P.S. & Soltis, D.E. (2000) The role of genetic and genomic attributes in the success of polyploids. *Proceedings of the National Academy of Sciences, USA*, 97, 7051–7057.
- Still, C.J., Berry, J.A., Collatz, G.J. & DeFries, R.S. (2003) Global distribution of C<sub>3</sub> and C<sub>4</sub> vegetation: carbon cycle implications. *Global Biogeochemical Cycles*, 17(1), 6–16.
- Tazoe, Y., Noguchi, K. & Terashima, I. (2006) Effects of growth light and nitrogen nutrition on the organization of the photosynthetic apparatus in leaves of a C<sub>4</sub> plant, *Amaranthus cruentus*. *Plant, Cell & Environment*, 29, 691–700.
- Valladares, F., Balaguer, L., Martinez-Ferri, E., Perez-Corona, E. & Manrique, E. (2002) Plasticity, instability and canalization: is the phenotypic variation in seedlings of sclerophyll oaks consistent with the environmental unpredictability of Mediterranean ecosystems? *New Phytologist*, 156, 457–467.
- Valluru, R., Gazave, E.E., Fernandes, S.B., Ferguson, J.N., Lozano, R., Hirannaiah, P. et al. (2019) Deleterious mutation burden and its association with complex traits in sorghum (*Sorghum bicolor*). *Genetics*, 211, 1075–1087.
- Vyas, P., Bisht, M.S., Miyazawa, S.-I., Yano, S., Noguchi, K., Terashima, I. et al. (2007) Effects of polyploidy on photosynthetic properties and anatomy in leaves of *Phlox drummondii*. *Functional Plant Biology*, 34, 673–682.
- Warner, D.A. & Edwards, G.E. (1989) Effects of polyploidy on photosynthesis rates, photosynthetic enzymes, contents of DNA, chlorophyll, and sizes and numbers of photosynthetic cells in the C<sub>4</sub> dicot *Atriplex confertifolia*. *Plant Physiology*, 91, 1143–1151.
- Warner, D.A., Ku, M.S.B. & Edwards, G.E. (1987) Photosynthesis, leaf anatomy, and cellular constituents in the polyploid C<sub>4</sub> grass *Panicum virgatum*. *Plant Physiology*, 84, 461–466.
- Warton, D.I., Duursma, R.A., Falster, D.S. & Taskinen, S. (2012) SMATR 3—an R package for estimation and inference about allometric lines. *Methods in Ecology and Evolution*, 3, 257–259.
- Witkowski, E.T.F. & Lamont, B.B. (1991) Leaf specific mass confounds leaf density and thickness. *Oecologia*, 88, 486–493.
- Wright, I.J., Reich, P.B., Cornelissen, J.H.C., Falster, D.S., Groom, P.K., Hikosaka, K. et al. (2005) Modulation of leaf economic traits and trait relationships by climate. *Global Ecology and Biogeography*, 14, 411–421.
- Wright, I.J., Reich, P.B., Westoby, M., Ackerly, D.D., Baruch, Z., Bongers, F. et al. (2004) The worldwide leaf economics spectrum. *Nature*, 428, 821–827.

Xiong, D. & Flexas, J. (2018) Leaf economics spectrum in rice: leaf anatomical, biochemical, and physiological trait trade-offs. *Journal of Experimental Botany*, 69, 5599–5609.

#### SUPPORTING INFORMATION

Additional supporting information can be found online in the Supporting Information section at the end of this article.

**How to cite this article:** Li, S., Moller, C. A., Mitchell, N. G., Martin, D. G., Sacks, E. J., Saikia, S., et al. (2022) The leaf economics spectrum of triploid and tetraploid C4 grass *Miscanthus x giganteus*. *Plant, Cell & Environment*, 45, 3462–3475. <https://doi.org/10.1111/pce.14433>